JACS
JOURNAL OF THE AMERICAN CHEMICAL SOCIETY

COMMUNICATION

pubs.acs.org/JACS

Stack Exchange Strategies for the Synthesis of Covalent Double-Channel Photosystems by Self-Organizing Surface-Initiated Polymerization

Naomi Sakai* and Stefan Matile*

Department of Organic Chemistry, University of Geneva, Geneva, Switzerland

Supporting Information

ABSTRACT: Ring-opening disulfide exchange polymerization has recently been identified as ideal for synthesizing single-channel photosystems by self-organizing surface-initiated polymerization (SOSIP). Here we introduce chemoorthogonal hydrazone exchange chemistry to engineer additional channels into single-channel photosystems. Post-SOSIP stack exchange is shown to provide facile access to complete supramolecular n/p-heterojunction architectures with high activity and freely variable composition, including oriented antiparallel redox gradients. With appropriate templation from the surface, post-SOSIP stack exchange is nearly quantitative.

Although they are essential for building the materials of the future, general approaches to covalent multichannel architectures on solid surfaces that are both oriented and ordered have remained beyond reach for decades.[1] This is understandable because of the formidable challenges in synthetic organic, supramolecular, and analytical chemistry involved. Current solution-processing methods for building optoelectronic devices naturally lack directionality.[2] Available approaches to build directly on the surface, such as layer-by-layer assembly, give little axial and no lateral organization.[3] The alternative zipper assembly has been successful in building supramolecular n/p-heterojunctions with oriented double-channel gradients,[4] but the synthetic efforts involved are much too demanding for general use, and covalent capture studies have failed.[5] Classical polymer brushes seem to stop growing as soon as the involved chemistry becomes more ambitious.[6]

Self-organizing surface-initiated polymerization (SOSIP) has recently been introduced as a promising method that applies lessons from nature to secure facile access to oriented and ordered single-channel architectures on solid surfaces.[7] However, supramolecular n/p-heterojunction (SHJ) photosystems require the coaxial alignment of two molecular-level pathways that can transport holes and electrons in opposite directions after their separation with light at the maximized n/p interface.[1,4] Lateral self-sorting during co-SOSIP is currently being explored as a supramolecular approach to SHJs.[8] This attractive approach is likely to be successful also in practice. However, it is less likely to obtain the experimental evidence to prove the occurrence of perfectly alternate lateral and uniform axial self-sorting during co-SOSIP. To build SOSIP architectures with confirmed coaxial channels at molecular-level resolution, covalent approaches will be unavoidable. In this communication, post-SOSIP stack exchange is introduced to tackle this challenge. In this general strategy, chemoorthogonal hydrazone exchange is employed after SOSIP to drill large pores next to the existing π-stacks and fill them with the complementary π-stacks (Figure 1).

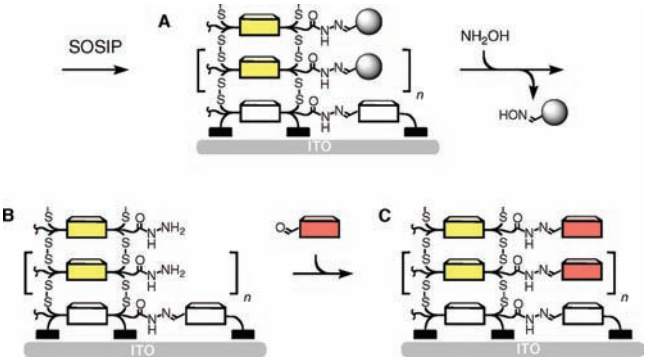

Figure 1. The concept of post-SOSIP stack exchange. Chemoorthogonal to the disulfide exchange chemistry used for SOSIP, hydrazone exchange chemistry is used to replace noninterfering and inactive domains (shaded circles in A) with active π-stacks (red boxes in C). For full structures, see Scheme 1.

In initiator **1** and propagators **2**, all that is needed for SOSIP is preserved (Scheme 1).[7] Both contain central naphthalenediimides (NDIs).[9] To direct their assembly into charge-transporting π-stacks, flanking hydrogen-bonded networks were inserted on both sides before the polymerizing subunits. Acyl hydrazones were placed in the self-organizing subunits of propagators **2** to place exchangeable subunits for the installation of additional charge-transporting channels by post-SOSIP stack exchange (Figure 1 and Scheme 1). In initiator **1**, the same hydrazones were used to link the NDI templates and diphosphonate "feet" to the central unit.

Initiator **1** and propagators **2** were prepared by reacting hydrazides **3** and **4** with aldehydes **5** and **6**, respectively. The synthesis of building blocks **3**−**5** from commercial starting materials is described in the Supporting Information (SI).[10]

Initiator **1** contains four diphosphonate feet for "tetravalent" binding to the ITO surface to firmly preorganize both SOSIP and the exchangeable subunit. The protecting groups on the surface of monolayer **7** (Figure S2 in the SI) were removed with dithiothreitol (DTT) to afford thiolates on the surface of monolayer **8**

Received: August 11, 2011
Published: October 25, 2011

Scheme 1. Synthesis of Covalent Double-Channel Photosystems by SOSIP and Stack Exchange[a]

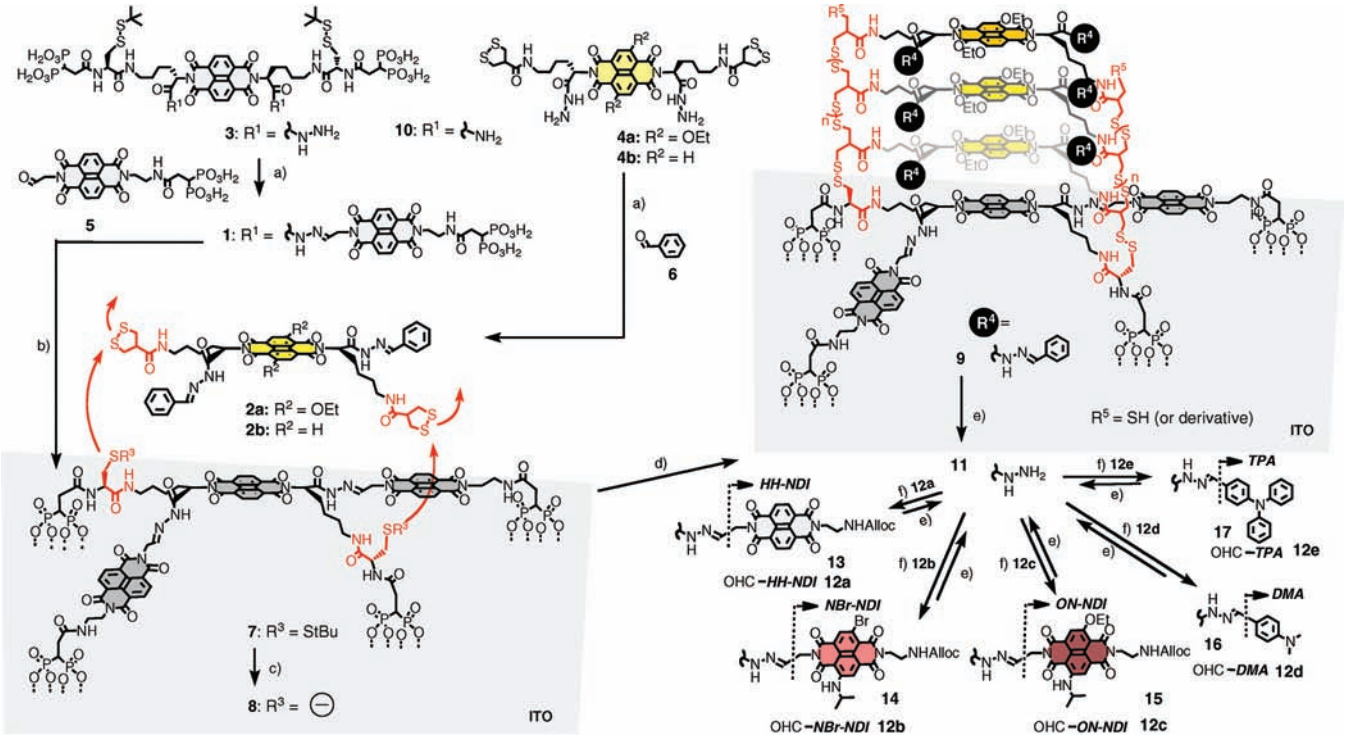

[a] Conditions: (a) TFA. (b) (1) **1**, DMSO, ITO; (2) 1 h, 120 °C. (c) DTT. (d) **2a**, 1:1 $CHCl_3$/MeOH, iPr_2NEt. (e) NH_2OH HCl, H_2O, (f) aldehyde, TFA or AcOH. See Figure S1 for the complete chemical structures. Dotted lines from the diphosphonate groups indicate the bonds to the ITO surface. **12b**, **12c**, **14**, and **15** are mixtures of 2,6- and 3,7-regioisomers; polymer structures are speculative generalized structures that are consistent with the experimental results. They naturally contain some defects, and the nature of the presumably oxidized thiol termini (R^5) at the surface is unknown.

(Scheme 1c). Propagator **2a** and a base catalyst were added next to initiate SOSIP (Scheme 1d). Molecular recognition by NDI stacking and hydrogen bonding was expected to place the strained disulfides from asparagusic acid in propagator **2a** on top of the thiolates of **8** to initiate ring-opening disulfide exchange[11,12] polymerization and produce SOSIP photosystem **9**.

SOSIP was followed by the increase in the 470 nm absorption of the yellow NDI from the propagator **2a** bound to the ITO surface. Under the optimized conditions, the onset of SOSIP occurred at a critical concentration $c_{SOSIP} \approx 7$ mM (Figure S3A). Competing polymerization in solution was not observed under these conditions. Replacement of the benzaldehyde hydrazones in propagator **2a** by acetone hydrazones made the eventual SOSIP indistinguishable from polymerization in solution (Scheme S2 and Figure S3C). The same was true for initiator **10** containing only two diphosphonate feet and primary amides in place of the templating NDI diphosphonates (Figure S3A, × symbols).

Stack exchange within the resulting SOSIP photosystem **9** was initiated by hydrazone−oxime exchange using excess hydroxylamine (Scheme 1e). The chemoorthogonality of disulfide and hydrazone exchange has been demonstrated extensively.[11,13] The hydrazide-rich pores drilled into the resulting architecture **11** were then filled by reversible covalent capture of various aldehydes (e.g., **12a**−**e**) to give hydrazones **13**−**17** (Scheme 1f).

Post-SOSIP stack exchange was monitored by the change in absorption of the coated ITO electrode (Figure 2). On the functional level, post-SOSIP stack exchange was characterized by photocurrent generation upon irradiation of the photosystem

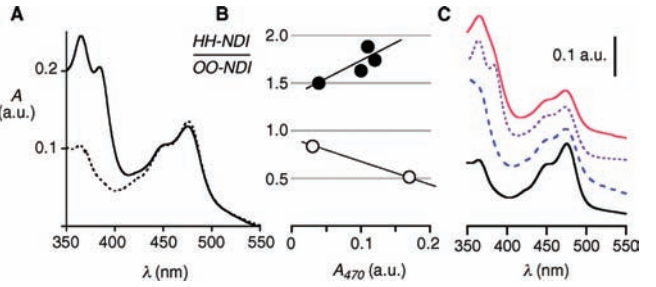

Figure 2. (A) Absorption spectra of photosystem **9** (dotted) and **13** (solid). (B) Molar ratio of colorless HH-NDIs from **12a** and yellow OO-NDIs from **2a** as a function of the thickness of photosystem **13** (●, A_{470} = 0.1 au ≈ 30 nm or 110 π-stacks).[10] For comparison, data for the control system **13′** made from template-free initiator **10** are also shown (○). (C) Changes in absorption spectra in response to stack exchange from **9** (black solid line) to **16** (blue dashed line), **13** (purple dotted line), and **17** (red solid line).

used as a working electrode in the presence of mobile triethanolamine hole acceptors, a Pt wire as a counter electrode, and Ag/AgCl as a reference electrode (Figure 3). The unchanged photocurrent and absorption after several on−off cycles of irradiation confirmed the stability of the photosystems under these conditions.

The exchange of the benzaldehyde hydrazones in photosystem **9** with the NDI stacks in photosystem **13** was correctly reflected by the appearance of a strong NDI absorption at 380 nm (Figure 2A). According to their extinction coefficients

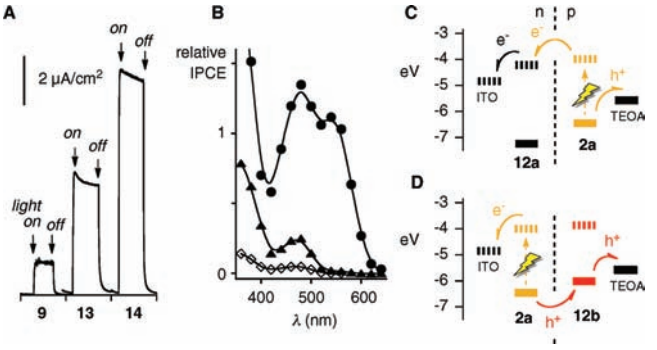

Figure 3. (A) Photocurrent generated by photosystems **9**, **13**, and **14** upon irradiation by a solar simulator (66 mW/cm^2). (B) Photocurrent action spectra of photosystems **9** (◊), **13** (▲), and **14** (●). (C, D) HOMO (bold) and LUMO (dotted) energy levels for photosystems (C) **13** and (D) **14** (in eV vs vacuum).

in solution, the molar ratio of unsubstituted and yellow NDIs could be calculated from changes in A_{380} and A_{470} (● data in Figure 2B). The obtained value of 1.7 ± 0.2 indicated that subunit exchange from photosystem **9** to photosystem **13** was almost quantitative.

Control experiments with SOSIP photosystems grown from initiator **10** revealed very little binding of NDI aldehyde **12a** (○ data in Figure 2B; also see Figure S7). Quite remarkably, the yield of templated post-SOSIP stack exchange changed little with increasing thickness of the photosystem, whereas that of untemplated post-SOSIP stack exchange became even poorer (Figure 2B). This sensitivity to the structure of the initiator demonstrates the central importance of the NDI diphosphonate hydrazones in initiator **1** as a template on the surface to secure the space needed for SOSIP of bulky propagators such as **2a** as well as for operational post-SOSIP stack exchange. These results are in excellent agreement with the formation of ordered ladderphane-like[14] structures by SOSIP (Scheme 1).

Consistent with the well-known chemoorthogonality of disulfide and hydrazone exchange reactions, post-SOSIP stack exchange could be repeated many times without significant loss of polymeric material (Figure 2C and Figure S6).

Post-SOSIP stack exchange from photosystem **9** to photosystem **13** caused a large increase in photocurrent generation (Figure 3A). This improved performance was as expected for a formal SHJ architecture, where coaxial stacks of yellow and unsubstituted NDIs can transport holes and electrons, respectively, and photoinduced charge separation can occur at the maximized molecular-level interface between the stacks.[1,4] The increased activity of yellow NDIs found at 470 nm in the photocurrent action spectra upon exchange from **9** to **13** (Figure 3B) is in agreement with this interpretation.

The exchange of stacks of unsubstituted NDIs in photosystem **13** with stacks of red NDIs in photosystem **14** nearly doubled the photocurrent generation (Figure 3A). In double-channel SHJ **14**, the red NDI stacks were expected to serve as p channels, whereas the yellow stacks should transport electrons (Figures 3D and 4A). Post-SOSIP stack exchange from SHJ **13** to **14** should occur with umpolung of the yellow NDI stacks from p to n transporters. This "ambipolar" behavior of yellow NDI stacks is consistent with their ability to undergo symmetry-breaking photoinduced charge separation (i.e., disproportionation into oxidized and reduced radicals) in response to irradiation with light.[7]

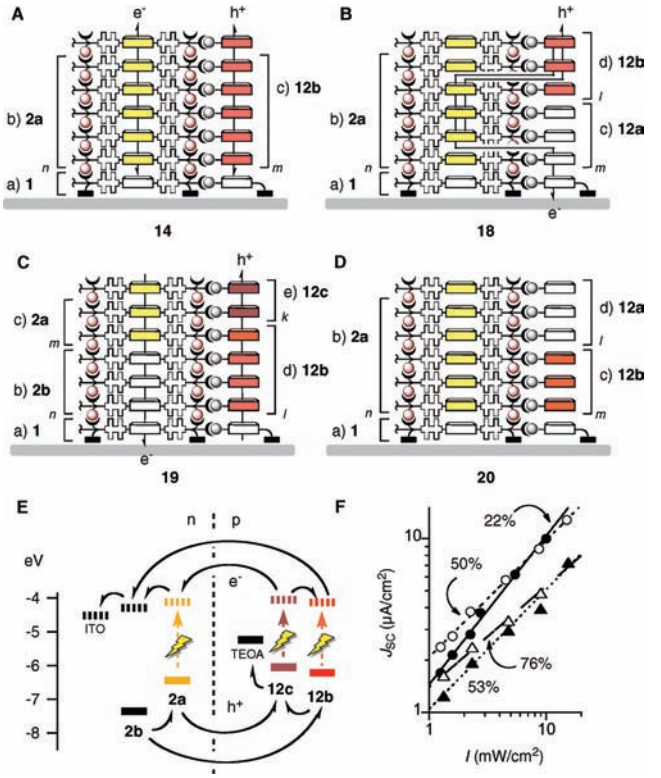

Figure 4. Schematic structures of (A) SHJ **14**, (B) three-component OMARG SHJ **18**, (C) four-component OMARG SHJ **19**, and (D) anti-OMARG SHJ **20** (a−e show the sequence of construction; see Schemes S6 and S7 for details). (E) HOMO and LUMO levels for **19**. (F) Dependence of the short-circuit current density (J_{SC}) on the light intensity (I) for **19** (●), **14** (○), **18** (▲), and **20** (△). Bimolecular charge recombination efficiencies η_{BR} are also shown.

Post-SOSIP stack exchange with other aldehydes, including more electron-rich NDIs **12c**, known hole conductors **12d** and **12e**, and electron-poor cyano NDIs gave clearly less active photosystems (Figures S9 and S10).

The three-component photosystem **18** was constructed from SHJ photosystem **13** with a central yellow π-stack of length n (Figures 2 and 4B). About half of the adjacent π-stacks formed by the unsubstitued NDIs **12a** was removed with hydroxylamine. The resulting pores were filled with red NDI aldehyde **12b** to give red π-stacks (from **12b**) of length l on top of colorless π-stacks (from **12a**) of length m (Figure 4B). All processes were followed quantitatively by absorption spectroscopy ($l \approx m$, $l + m \approx n$; Figure 4B and Figure S8A).[10]

The four-component system **19** was produced analogously from **8** by successive SOSIP of **2b** and **2a** (with $n \approx m$) followed first by complete stack exchange with **12b** and then by partial stack exchange with **12c** (with $l \approx 20k$ because of the poor intrinsic activity of the ON-NDIs in **12c**; Figure 4C and Figure S8B).[10] **19** possesses clearly separated electron- and hole-conducting pathways, both equipped with redox gradients (Figure 4E). This system resembles the previously reported SHJ with oriented multicolored antiparallel redox gradients (OMARG), which was shown to generate more photocurrent than the one without gradients because of the minimized charge recombination.[4] On the other hand, the three-component system **18** is a new type of OMARG in which, as a result of the ambipolar nature of the yellow NDI stacks, two conducting

pathways partially overlap. The misaligned three-component anti-OMARG SHJ **20**, in which the position of the red and unsubstituted NDIs in **18** is switched, was also assembled by partial stack exchange from **14** to assess the significance of this novel construct ($l \approx m$; Figure 4D and Figure S8C).

The effect of redox gradients was clearly seen in the dependence of the short-circuit current density J_{SC} on the light intensity I (Figure 4F). Their relationship is often described by the equation $J_{SC} \propto I^{\alpha}$. The exponent α has been shown to be related to the bimolecular recombination loss efficiency η_{BR} (the fraction of charges lost by recombination) by the equation $\eta_{BR} = \alpha^{-1} - 1$.[15] As expected, the lowest η_{BR} was found for the systems with correctly oriented antiparallel redox gradients in the two channels (22 ± 3% for **19**; ● in Figure 4F). The lower η_{BR} obtained for **18** (53 ± 8%; ▲ in Figure 4F) in comparison with its constitutional isomer **20** (76 ± 8%; △ in Figure 4F) is in agreement with the favorable effect of the gradient in minimizing charge recombination and supports the occurrence of partial hydrazone exchange from the surface of the film. On the other hand, the η_{BR} obtained for three-component OMARG SHJ **18** was significantly higher than that for four-component OMARG SHJ **19** and almost the same as that of simple SHJ **14** (50 ± 3%; ○ in Figure 4F). These results demonstrate that double-channel redox gradients are needed to minimize the loss of charges.

Taken together, our results show that stack exchange in SOSIP architectures can be considered as a unique, reliable, and general approach for building ordered and oriented multicomponent systems of appreciable sophistication in a straightforward, user-friendly manner. Our current objective is to maximize the complexity accessible by subunit exchange on the one hand and to explore the potential for practical applications on the other.

■ ASSOCIATED CONTENT

Supporting Information. Details of experimental procedures and additional results. This material is available free of charge via the Internet at http://pubs.acs.org.

■ AUTHOR INFORMATION

Corresponding Author
Naomi.Sakai@unige.ch; Stefan.Matile@unige.ch

■ ACKNOWLEDGMENT

We thank D. Jeannerat, A. Pinto, and S. Grass for NMR measurements; the Sciences Mass Spectrometry (SMS) Platform for mass spectrometry services; and the University of Geneva, the European Research Council (ERC Advanced Investigator), the National Centre of Competence in Research (NCCR) in Chemical Biology, and the Swiss NSF for financial support.

■ REFERENCES

(1) (a) Würthner, F.; Meerholz, K. *Chem.—Eur. J.* **2010**, *16*, 9366. (b) Wasielewski, M. R. *Acc. Chem. Res.* **2009**, *42*, 1910. (c) Bassani, D. M.; Jonusauskaite, L.; Lavie-Cambot, A.; McClenaghan, N. D.; Pozzo, J.-L.; Ray, D.; Vives, G. *Coord. Chem. Rev.* **2010**, *254*, 2429. (d) Bhosale, R.; Míšek, J.; Sakai, N.; Matile, S. *Chem. Soc. Rev.* **2010**, *39*, 138.

(2) (a) Sugiyasu, K.; Kawano, S.; Fujita, N.; Shinkai, S. *Chem. Mater.* **2008**, *20*, 2863. (b) Jonkheijm, P.; Stutzmann, N.; Chen, Z.; de Leeuw, D. M.; Meijer, E. W.; Schenning, A. P. H. J.; Würthner, F. *J. Am. Chem. Soc.* **2006**, *128*, 9535. (c) Li, W.; Saeki, A.; Yamamoto, Y.; Fukushima, T.; Seki, S.; Ishii, N.; Kato, K.; Takata, M.; Aida, T. *Chem.—Asian J.* **2010**, *5*, 1566. (d) Bu, L.; Guo, X.; Yu, B.; Qu, Y.; Xie, Z.; Yan, D.; Geng, Y.; Wang, F. *J. Am. Chem. Soc.* **2009**, *131*, 13242.

(3) (a) Decher, G. *Science* **1997**, *277*, 1232. (b) Mwaura, J. K.; Pinto, M. R.; Witker, D.; Ananthakrishnan, N.; Schanze, K. S.; Reynolds, J. R. *Langmuir* **2005**, *21*, 10119. (c) Guldi, D. M. *J. Phys. Chem. B* **2005**, *109*, 11432. (d) Kira, A.; Umeyama, T.; Matano, Y.; Yoshida, K.; Isoda, S.; Park, J. K.; Kim, D.; Imahori, H. *J. Am. Chem. Soc.* **2009**, *131*, 3198.

(4) Sakai, N.; Bhosale, R.; Emery, D.; Mareda, J.; Matile, S. *J. Am. Chem. Soc.* **2010**, *132*, 6923.

(5) Sakurai, S.; Areephong, J.; Bertone, L.; Lin, N.-T.; Sakai, N.; Matile, S. *Energy Environ. Sci.* **2011**, *4*, 2409.

(6) (a) Snaith, H. J.; Whiting, G. L.; Sun, B.; Greenham, N. C.; Huck, W. T. S.; Friend, R. H. *Nano Lett.* **2005**, *5*, 1653. (b) Foster, S.; Finlayson, C. E.; Keivanidis, P. E.; Huang, Y.-S.; Hwang, I.; Friend, R. H.; Otten, M. B. J.; Lu, L.-P.; Schwartz, E.; Nolte, R. J. M.; Rowan, A. E. *Macromolecules* **2009**, *42*, 2023.

(7) Sakai, N.; Lista, M.; Kel, O.; Sakurai, S.; Emery, D.; Mareda, J.; Vauthey, E.; Matile, S. *J. Am. Chem. Soc.* **2011**, *133*, 15224.

(8) Lista, M.; Areephong, J.; Sakai, N.; Matile, S. *J. Am. Chem. Soc.* **2011**, *133*, 15228.

(9) Sakai, N.; Mareda, J.; Vauthey, E.; Matile, S. *Chem. Commun.* **2010**, *46*, 4225.

(10) See the SI.

(11) (a) Corbett, P. T.; Leclaire, J.; Vial, L.; West, K. R.; Wietor, J.-L.; Sanders, J. K. M.; Otto, S. *Chem. Rev.* **2006**, *106*, 3652. (b) Skene, W. G.; Lehn, J.-M. *Proc. Natl. Acad. Sci. U.S.A.* **2004**, *101*, 8270.

(12) (a) Krisovitch, S. M.; Regen, S. L. *J. Am. Chem. Soc.* **1992**, *114*, 9828. (b) Carnall, J. M. A.; Waudby, C. A.; Belenguer, A. M.; Stuart, M. C. A.; Peyralans, J. J.; Otto, S. *Science* **2010**, *327*, 1502. (c) Otto, S.; Furlan, R. L. E.; Sanders, J. K. M. *Science* **2002**, *297*, 590. (d) Anfinsen, C. B. *Science* **1973**, *181*, 223. (e) Mindell, J. A.; Zhan, H.; Huynh, P. D.; Collier, R. J.; Finkelstein, A. *Proc. Natl. Acad. Sci. U.S.A.* **1994**, *91*, 5272. (f) Prins, L. J.; Scrimin, P. *Angew. Chem., Int. Ed.* **2009**, *48*, 2288.

(13) (a) Rodriguez-Docampo, Z.; Otto, S. *Chem. Commun.* **2008**, 5301. (b) von Delius, M.; Geertsema, E. M.; Leigh, D. A. *Nat. Chem.* **2010**, *2*, 96.

(14) Chou, C.-M.; Lee, S.-L.; Chen, C.-H.; Biju, A. T.; Wang, H.-W.; Wu, Y.-L.; Zhang, G.-F.; Yang, K.-W.; Lim, T.-S.; Huang, M.-J.; Tsai, P.-Y.; Lin, K.-C.; Huang, S.-L.; Chen, C.; Luh, T.-Y. *J. Am. Chem. Soc.* **2009**, *131*, 12579.

(15) Koster, L. J. A.; Kemerink, M.; Wienk, M. M.; Maturová, K.; Janssen, R. A. J. *Adv. Mater.* **2011**, *23*, 1670.